Enhanced Electrochromism with Rapid Growth Layer-by-Layer Assembly of Polyelectrolyte Complexes

*Mengqi Cui, Wee Siang Ng, Xu Wang, Peter Darmawan, and Pooi See Lee**

In this work, a facile method to deposit fast growing electrochromic multilayer films with enhanced electrochemical properties using layer-by-layer (LbL) self-assembly of complex polyelectrolyte is demonstrated. Two linear polymers, poly(acrylic acid) (PAA) and polyethylenimine (PEI), are used to formulate stable complexes under specific pH to prepare polyaniline (PANI)/PAA-PEI multilayer films via LbL deposition. By introducing polymeric complexes as building blocks, $[PANI/PAA-PEI]_n$ films grow much faster compared with $[PANI/PAA]_n$ films, which are deposited under the same condition. Unlike the compact $[PANI/PAA]_n$ films, $[PANI/PAA-PEI]_n$ films exhibit porous structure that is beneficial to the electrochemical process and leads to improved electrochromic properties. An enhanced optical modulation of 30% is achieved with $[PANI/PAA-PEI]_{30}$ films at 630 nm compared with the lower optical modulation of 11% measured from $[PANI/PAA]_{30}$ films. The switching time of $[PANI/PAA-PEI]_{30}$ films is only half of that of $[PANI/PAA]_{30}$ films, which indicates a faster redox process. Utilizing polyelectrolyte complexes as building blocks is a promising approach to prepare fast growing LbL films for high performance electrochemical device applications.

1. Introduction

Electrochromic (EC) materials comprise redox-active species that exhibit significant, lasting and reversible changes upon coloration when electrons and cations such as H^+ or Li^+ are injected or withdrawn reversibly. These small ions intercalation/de-intercalation within the active material matrix widens/narrows the electronic band gap, resulting in differing wavelength absorptions, thus displaying the complimentary visible or non-visible wavelengths. For example, an electrochromic material can switch from a clear form to a colored form when it is oxidized, or vice versa.

Unlike light emitting diodes which are associated with active emissive mechanism, the operation of devices utilizing electrochromic materials are based on non-emissive reflective or transmissive mechanism in which the visual effects are accounted by modulation of light. Moreover, electrochromic materials need only an initial current pulse at a sufficient driving potential to excite the electrochemical reaction, which requires low power consumption.[1] Thus electrochromic materials are promising for non-emissive display and energy conservation applications, such as electronic paper, active thermal control system and smart windows for green buildings.[1,2]

Among different types of electrochromic materials, conjugated conducting polymers have attracted great interests.[3] Polyaniline (PANI), an important polymer that exhibits electrochromism, is capable of multiple redox transitions without the need of chemical derivatization of the monomer. Therefore, PANI offers a simple platform for polyelectrochromism. PANI films prepared by electrochemical deposition (ECD) from aniline and dopants solutions are widely studied and show stable switching between emeraldine salt (ES) and leucoemeraldine base (LB) states.[4] However, large area PANI films achieved by ECD require a comparable counter electrode to provide stable and uniformly distributed electric field, in order to achieve a uniform and conformal scaled-up film. Solution-processable PANI complexes can be obtained from oxidative polymerization of aniline in the presence of polymer acids.[5] However, films prepared by spin-coating of these complexes showed delayed kinetics, presumably because of the slow polymer acid dynamics.[6,7] An alternative approach is to fabricate polymeric EC films via layer-by-layer (LbL) self-assembly. Over the past decades, LbL self-assembly has been proved to be a versatile and facile method to fabricate layered thin films incorporating various functional materials, at the same time exerts precise control over the film composition and structure.[8,9] This technique is suitable for large area deposition on substrates with arbitrary shapes, without the requirement of complex set-up or the need of conducting substrates. The most commonly studied strategy for LbL EC films is based on the electrostatic interaction between polycations and polyanions.[10] Schlenoff first explored LbL films for electrochromic study using polyviologens and poly(sodium styrenesulfonate).[11] Hammond and co-workers successfully fabricated a switchable electrochromic device based on LbL assembly, with PANI/poly(2-acrylamido-methane-s-propanesulfonic acid) (PAMPS) multilayers as one electrode and poly(3,4-ethylenedioxythiophene)-poly(styrene sulfonated) (PEDOT:PSS)/linear poly(ethylene imine) (LPEI) as the complementary electrode.[12] Thereafter, many other electrochromic multilayer films have been fabricated and studied, including polymeric films such

M. Cui, W. S. Ng, X. Wang,
Dr. P. Darmawan, Prof. P. S. Lee
School of Materials Science and Engineering
Nanyang Technological University
50 Nanyang Avenue, Singapore 639798
E-mail: pslee@ntu.edu.sg

DOI: 10.1002/adfm.201402100

as PANI/PSS,[13] PANI/poly(vinyl sulfonate)[14] and PANI/poly(acrylic acid) films;[15] polymer-inorganic hybrid films such as PANI/Prussian Blue and PANI/V_2O_5 multilayers;[16,17] and films with incorporation of carbon materials, which could benefit electrons transfer in the films, such as PANI/GO.[18] Recently, Lu and co-workers synthesized starlike polyaniline-tethered silsesquioxane (POSS-PANI) nanocage, and fabricated $(POSS\text{-}PANI/PAMPS)_n$ and $(POSS\text{-}PANI/sulfonated\text{-}PANI)_n$ films.[19] These films showed promising electrochromic properties, with enhanced contrast compared with normal PANI films and elevated kinetics compared to films deposited via other methods such as spin coating. The improvement was attributed to the loosely packing structure introduced by the starlike molecular architecture of POSS-PANI and the unique morphology created by LbL assembly. However, this kind of LbL approach usually suffers from slow process (<20 nm h^{-1}) and requires quite long time for the film preparation. Tens and even hundreds of layers need to be deposited in order to incorporate enough active materials for demanding optical modulation.[7,8,12]

Several methods have been explored to speed up the process of LbL assembly. Spin-coating assisted LbL and spray-coating assisted LbL are developed to fabricate thick films in a short time instead of traditional dip-coating LbL procedure.[20] However, these two methods are not suitable for non-planar substrates, and the film morphology may also differ from the one made by dip-coating LbL assembly.[21] The high spin speed in spin-coating and high pressure on the film surface in the spray-coating will influence the surface morphology of the film. Rapid growth of multilayer films could also be achieved when the films show exponentially growth behavior.[22] However, the exponential film growth behavior usually happens when certain kind of components are incorporated, such as weak polyelectrolytes, which possess high mobility and could easily diffuse in-and-out throughout the film under specific pH values.[23,24] Recently, the use of polymeric complexes as novel building blocks is considered to be a promising method to fabricate LbL films rapidly, at the same time possess the merits of traditional dip-coating LbL method.[25] Polymeric complexes are formed by the complexation of different polymers. The driving force includes electrostatic interaction between polycations and polyanions, hydrogen-bonding between donors and acceptors, guest-host interactions and so forth.[26,27] Nonstoichiometric polymeric complexes possess abundant uncoordinated groups on the outer surface, thus these groups could interact well with complementary species to fabricate multilayer films via LbL assembly. The large dimensions of the polymeric complexes and relatively large amount of charges they carry compared to the individual polymers possibly lead to the rapid growth of LbL films during the deposition.[27,28] The special spatial structures and the diverse components of polymeric complexes also hold promise of constructing films with tailored structures and multi-function, which could not be easily achieved by using individual polymer component.[25] The group of Sun successfully fabricated porous films up to 3 μm within 20 deposition cycles by using PAA-diazoresin (DAR) and PSS-DAR complexes.[28] They further developed rapid fabrication of LbL films with hierarchical micro- and nanostructure using poly(vinylpyrrolidione) (PVPON)-PAA complexes and poly(methacrylic acid) (PMAA) as building blocks. This kind of film could be easily developed as superhydrophobic coating benefiting from its unique morphology.[27] Even though the usage of polymeric complexes has attracted lots of interests, the advantage of using them in electrochemically functional films has not been exploited. Noting the potential to enhance electrochemical kinetics with the porous structures and the rapid film growth rates, it is of great interest to exploit the potential of polymeric complex for electrochromics and realize its superior electrochemical performance.

In this work, we demonstrate the rapid fabrication of LbL EC films by alternatively depositing negatively charged polymeric complex PAA-PEI with PANI as electrochemical active material. We investigate the structure, morphology and rapid growth behavior of the LbL films. We further illustrate the benefits of having the complex as building blocks in LbL films during electrochemical reaction that gives desirable electrochromic properties compared with films fabricated by individual polymers.

2. Results and Discussion

2.1. Characterization of Polyelectrolyte Complexes

It is well-known that the intermediate oxidation state (emeraldine base, EB) of PANI can be protonated by small-molecule acids and lead to the formation of the green color, electrically conducting emeraldine salt (ES) form. In this work, the pH value of PANI aqueous solution was kept at 2.85. Under this condition, the amino groups of PANI were highly protonated, resulting in the formation of positively charged ES solution.[17,30] As PAA is a weak polyelectrolyte, its configuration highly depends on the pH of the solution. Under high pH, the carboxyl groups are dissociated and the polymer chains tend to be extended. On the contrary, under low pH environment the carboxyl groups of PAA are highly protonated, and the polymer chains tend to curl up and become more hydrophobic, which is favorable for forming porous structure during LbL process.[27,31] In this work, the formation of PAA-PEI complexes is driven by the electrostatic interaction between the protonated amino groups on PEI and the dissociated carboxylic acid groups on PAA. The pH values of both of the polyelectrolyte solutions and the ratio of the two components in the mixture are critical for the formation of stable PAA-PEI complexes. Once the PEI solution was added into PAA solution, the solution became turbid and large floccules could be observed. The formation of large floccules was caused by the uneven distribution of PEI in the solution and the strong electrostatic interaction between PEI and PAA. The floccules disappeared after all the PEI solution was added under vigorously stirring, indicating new equilibrium was established. The mixture was further stirred for 30 min in order to get stable PAA-PEI complex suspension. The size and ζ potential were measured by Nanosizer. The PAA-PEI complexes exhibited an average hydrodynamic diameter of 342.5 nm (cf. Supporting Information Figure S1), with ζ potential of –45.9 mV. The negative ζ potential indicated that PAA was the dominating component on the surface of the PAA-PEI complexes.

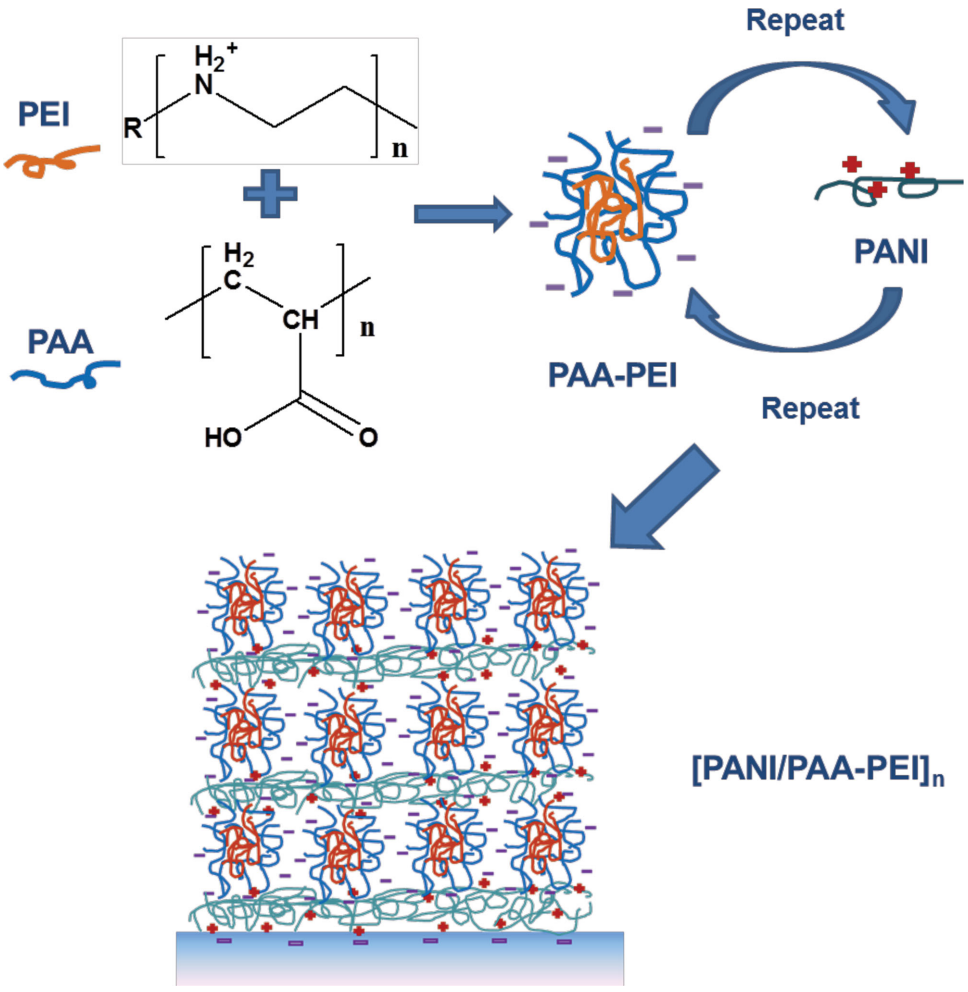

Figure 1. Schematic illustration of the structure of PAA-PEI complex and the process to fabricate LbL films.

2.2. Layer-by-Layer Assembly of Rapid Growing $[PANI/PAA-PEI]_n$ Multilayer Films

Multilayer films of PANI/PAA-PEI were deposited by alternatively dipping the substrate in PANI solution and PAA-PEI complexes suspension. **Figure 1** illustrated the structure of PAA-PEI complexes and the deposition procedure for PANI/PAA-PEI multilayers. In order to investigate the effect of polyelectrolyte complexes to the LbL films, PANI/PAA multilayer films were fabricated as control samples under the same conditions with PANI/PAA-PEI films. The driving force for LbL assembly was provided by the electrostatic interaction between cationic amino groups on the backbone of protonated PANI and those dissociated carboxylic acid groups on PAA and the surface of PAA-PEI complexes.[15,19,32]

Figure 2 shows the surface morphology and cross-sectional view of the $[PANI/PAA]_{20}$ film and the $[PANI/PAA-PEI]_{20}$ film. The $[PANI/PAA]_{20}$ film possesses compact structure (Figure 2a,b), while the film consisted of polyelectrolyte complexes displays obvious porous structures (Figure 2d,e). This porous structure originates from the relatively rigid structure of the electrostatically cross-linked PAA-PEI complexes and the strong electrostatic repulsion between the complexes, while the uncomplexed PAA is more flexible and tends to self-adjust its configuration to form a smooth surface during the deposition process.[28] The cross-section images (Figure 2c,f) show that the thickness of $[PANI/PAA-PEI]_{20}$ film is around 430 nm, which is obviously larger than the thickness of $[PANI/PAA]_{20}$ (which is around 200 nm) under the same deposition condition. UV–Vis absorbance spectra of $[PANI/PAA-PEI]_n$ and $[PANI-PAA]_n$ films with different deposition cycles further illustrate the process of film growth in the first 20 deposition cycles. As shown in **Figure 3**, the absorption peaks at about 320 nm are from excitation of the benzene segment on polyemeraldine chains. The peaks near 430 nm are due to the polaron absorption, and the peaks at around 600 nm are from the quinoid segment on partially protonated polyaniline chains.[19,33] The absorbance of the film increases as the deposition number increases, but the absorbance of the film with PAA-PEI complexes grows much faster than the film with individual PAA. **Figure 4**a shows the thickness of the films as a function of number of bilayers. The thickness of $[PANI/PAA-PEI]_n$ films grows exponentially with the number of deposition cycles, while the thickness of $[PANI/PAA]_n$ grows linearly. The dash lines indicate the exponential fit (in red) and linear fit (in black), respectively. The fast growth of polyelectrolyte complexes film can be attributed to the larger

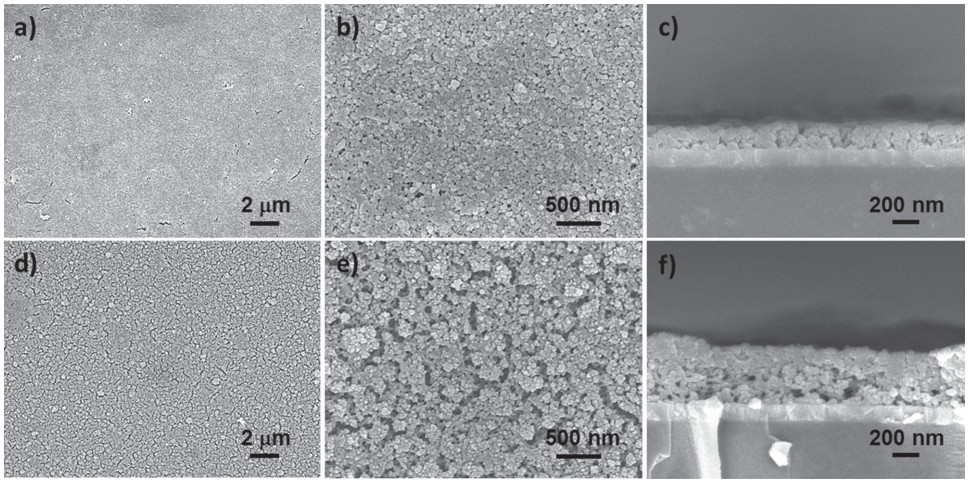

Figure 2. a,b) Top-view SEM images of the $[PANI/PAA]_{20}$ film; d,e) top-view SEM images of the $[PANI/PAA\text{-}PEI]_{20}$ film; cross-section image of c) the $[PANI/PAA]_{20}$ film, and f) the $[PANI/PAA\text{-}PEI]_{20}$ film.

dimensions of PAA-PEI complexes than pure PAA.[25] Avoiding intermediate drying step and tailoring specific pH of the dipping solutions also promote the loose packing of PAA-PEI complex and PANI.[27]

However, the well accepted "in-and-out" diffusion mechanism[34] for exponential growth behavior, which is based on the diffusion behavior of weak polyelectrolytes under restricted pH values, could not be fully applied on this $[PANI/PAA\text{-}PEI]_n$ system. Even though both PAA and PEI are weak polyelectrolytes, the pH of all the dipping solutions were kept at low values. Under this condition, the linear PEI was highly protonated and the mobility of PEI and PAA was restricted by the strong electrostatic interaction, which was not favorable for "in-and-out" diffusion.[24] Recently, Sun and co-workers proposed surface roughness induced exponential growth mechanism based on their study on LbL films composed of PVPON-PAA complexes.[27] They pointed out that with the increasing deposition cycles, the increased surface roughness led to increased surface area, which permitted more building blocks to be deposited on the film than in the previous deposition cycle. In our present work, the relatively large amount of charges carried by the PAA-PEI complexes cause strong repulsion between the complexes, which resulted in the uneven distribution of the complexes when they are adsorbed to the film surface. Thus the films show a porous structure with rough surface. The surface roughness of the films was monitored by AFM (cf. Supporting Information Figure S2). The root mean square roughness of the LbL films is shown in Figure 4b. It could be seen that the roughness of $[PANI/PAA\text{-}PEI]_n$ films grow distinctly with the increasing deposition cycles, while the surfaces of $[PANI/PAA]_n$ films are much smoother. For example, the root mean square roughness of the $[PANI/PAA\text{-}PEI]_{40}$ film is around 170 nm, while it is only around 50 nm for the $[PANI/PAA]_{40}$ film as measured using AFM. We therefore attribute that both the large dimensions of the polyelectrolyte complexes and the surface roughness induced exponential growth behavior contributed to the fast growth of $[PANI/PAA\text{-}PEI]_n$ films.

2.3. Electrochromic Properties of $[PANI/PAA\text{-}PEI]_n$ Films

Cyclic voltammetry of $[PANI/PAA]_{30}$ and $[PANI/PAA\text{-}PEI]_{30}$ films collected in 1 M $LiClO_4$ in PC are shown in **Figure 5**a and 5b, respectively. Two pairs of oxidation and reduction peaks could be recognized from the CV curves of both films under low scan rate. The oxidation peaks at lower potential are due to the leucoemeraldine to emeraldine state transition, and the oxidation peaks at higher potential can be assigned to the transition from emeraldine to pernigraniline state.[19,35] It could be observed that the transition between the emeraldine and pernigraniline state is shifted to lower potentials for $[PANI/PAA\text{-}PEI]_{30}$ films compared with $[PANI/PAA]_{30}$ films, which could be attributed to the existence of protonated PEI in the film. The substantial protons carried by PEI could affect the doping level of PANI and therefore regulates the electrochemical behavior of the LbL films. The contributions of protonated PEI are further illustrated in the discussion of EIS results and electrochromic characterizations. Under high scan rate, the potential separation between

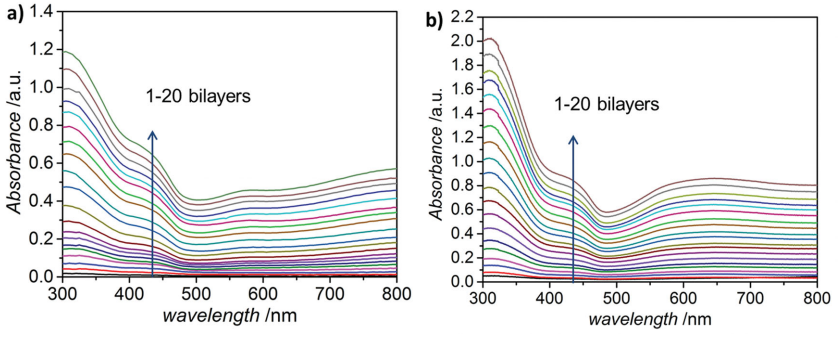

Figure 3. UV–Vis absorption spectra of a) $[PANI/PAA]_n$ multilayers and b) $[PANI/PAA\text{-}PEI]_n$ multilayers assembled on quartz slides.

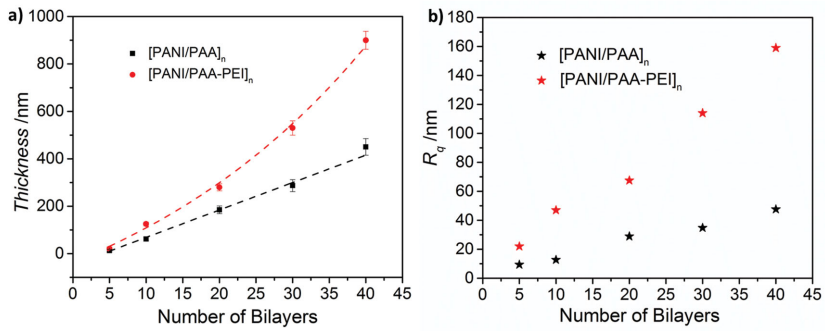

Figure 4. Dependence of the a) thickness, and b) roughness of the $[PANI/PAA]_n$ and $[PANI/PAA\text{-}PEI]_n$ films as a function of the deposition cycles.

the oxidation and the reduction peaks of $[PANI/PAA\text{-}PEI]_{30}$ is smaller than that of $[PANI/PAA]_{30}$, indicating a more favorable electrochemical reaction in $[PANI/PAA\text{-}PEI]_{30}$ films with better reaction reversibility. Because the two pairs of redox peaks of $[PANI/PAA\text{-}PEI]_{30}$ are near to each other and the width of the peaks are broad, the two pairs of redox peaks merge into one pair of wide redox peaks under high scan rate. Similar phenomenon is also observed in other reported LbL films.[19] The effective ion diffusion coefficient can be estimated by applying Randles Sevcik equation:[36,37]

$$I_{peak} = 2.71 \times 10^5 \times A \times C \times D^{1/2} n^{3/2} v^{1/2} \quad (1)$$

where I_{peak} stands for the peak current, A is the electrode area, C is the concentration of species in the bulk, D is the diffusion coefficient, n is the number of electrons involved in the redox reaction and υ is the scan rate. As shown in Equation 1, the I_{peak} is proportional to $\upsilon^{1/2}$, and the D can be extracted from the slope (cf. Supporting Information Figure S3). The improved ion diffusion coefficient in $[PANI/PAA\text{-}PEI]_{30}$ films compared to $[PANI/PAA]_{30}$ films illustrates fast ion diffusion process in the porous films.

Figure 6a,b shows the UV–Vis transmittance response of the $[PANI/PAA]_{30}$ and $[PANI/PAA\text{-}PEI]_{30}$ films under oxidized state and reduced state. The transmittance of $[PANI/PAA\text{-}PEI]_{30}$ is slightly lower than $[PANI/PAA]_{30}$ at all applied potentials, which is consistent with the difference in the film thickness. It is observed that the transmittance of both films decreases as the applied potential increases from –0.3 V to 0.9 V, where PANI is oxidized from LB state to PS state. The contrast ($\Delta T = T_b - T_c$, where T_b and T_c are denoted as transmittance at bleached and colored states, respectively) was extracted at 630 nm. As shown in Figure 6c, the contrast of the $[PANI/PAA\text{-}PEI]_{30}$ film could reach up to ΔT = 28.7%, while the contrast of the $[PANI/PAA]_{30}$ film is only ΔT = 11.1%. The transmittance modulation of $[PANI/PAA\text{-}PEI]_{30}$ is higher than other PANI/polymer based LbL films reported in the literature, such as $[PANI/PNACN]_{30}$ and $[POSS\text{-}PANI/PAMPS]_{50}$.[19,38] It has been suggested that the contrast of an electrochromic film is related to the amount of active material that can be intercalated with electrolyte ions.[2,39] The fast growing behavior of $[PANI/PAA\text{-}PEI]_n$ allows a large amount of active materials deposited into the film in a short time, while $[PANI/PAA]_n$ only incorporated limited amount of active materials under the same condition. On the other hand, the introduction of the PAA-PEI complexes into the film leads to porous structure, which provides large inner space of the films and ensures the interaction between PANI and electrolyte ions. These two characteristics of $[PANI/PAA\text{-}PEI]_n$ have contributed to the higher contrast.

Kinetics study was also conducted at 630 nm. The applied potential was switched between –0.3V and 0.9V. Switching time is described as 90% of the time taken for the completion of color conversion under kinetic test condition. For $[PANI/PAA]_{30}$ films, the coloration time is 6 s and the bleaching time is 24 s. Under the same condition, the films fabricated with PANI and PAA-PEI complexes display faster switching behavior with coloration time and bleaching time of 3 s and 15 s, respectively. The switching time could be affected by several factors such as film thickness, applied potential, ionic conductivity of electrolyte, and charge transfer resistivity.[40] Thick films usually result in longer switching behavior as the diffusion process is much slower than that in the thin films.[41] However, even though the $[PANI/PAA\text{-}PEI]_{30}$ is much thicker than the $[PANI/PAA]_{30}$ films in this work, the porous structure plays an important role in enhancing the switching kinetics.[2,40] It has been suggested that the electrochromic process involved double injection/extraction of electrons and ions from the film. In general, a compact film structure would lead to slow diffusion process and thus long switching time.[19] The highly porous structure of $[PANI/PAA\text{-}PEI]_n$ provides large reaction surface and inner space for electrolyte to penetrate into the film, thus shortening the ion diffusion pathways.[2,36,40,42] This result is in accordance with a larger ion diffusion coefficient of $[PANI/PAA\text{-}PEI]_{30}$ as discussed earlier. Polymer-based EC films with porous structure are usually fabricated using template or specific deposition conditions.[40,43] In this work, we show that porous EC films can also be fabricated by solution-processable method without any template or seed layers.

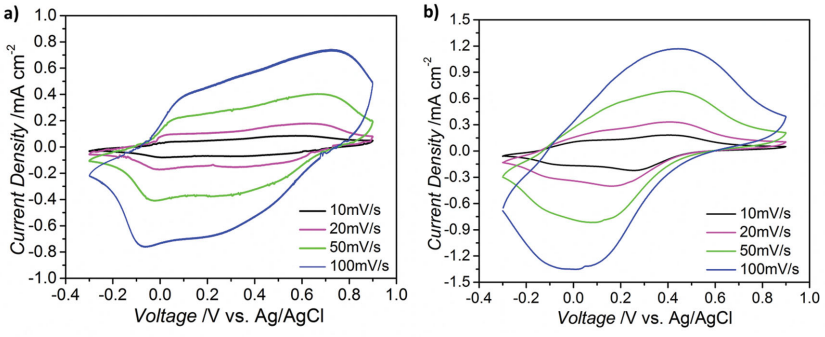

Figure 5. CV curves of the a) $[PANI/PAA]_{30}$ film and b) $[PANI/PAA\text{-}PEI]_{30}$ film under different scan rates in 1 M $LiClO_4$ in PC.

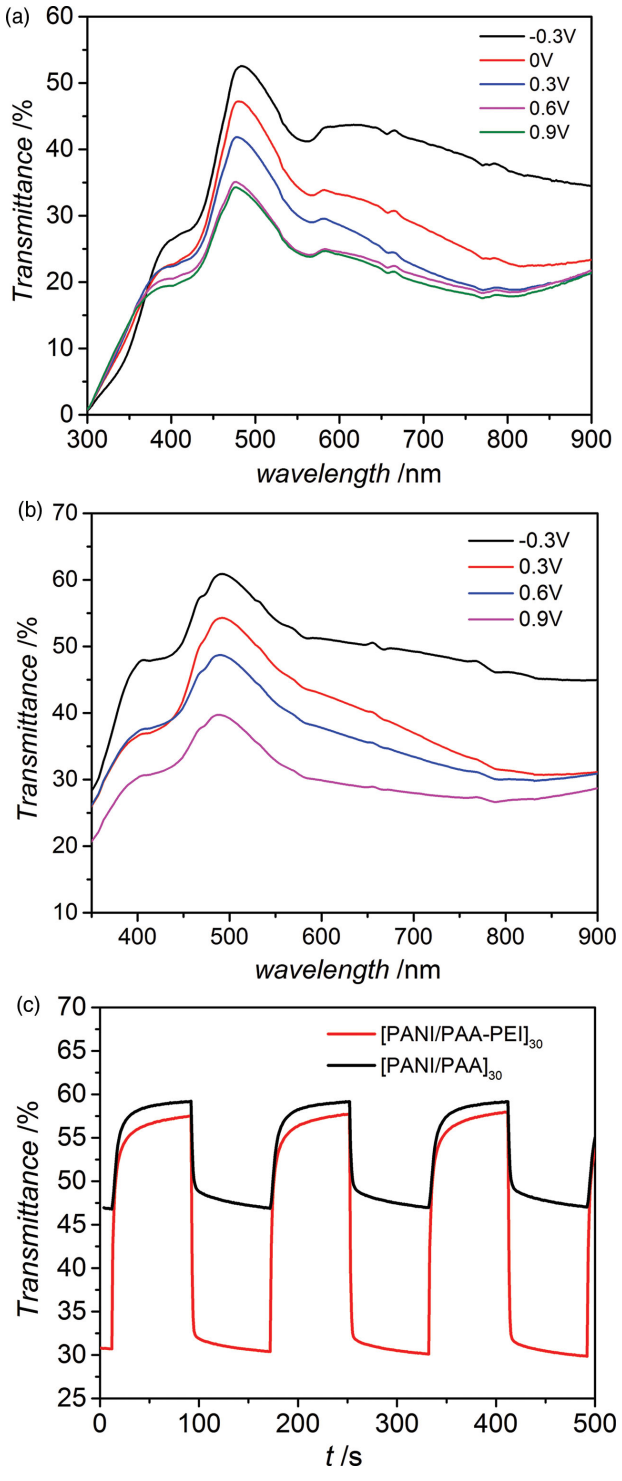

Figure 6. Electrochromic behaviors of the $[PANI/PAA]_{30}$ and $[PANI/PAA\text{-}PEI]_{30}$ films: a) UV–Vis spectra of $[PANI/PAA]_{30}$ under varying potentials; b) UV–Vis spectra of $[PANI/PAA\text{-}PEI]_{30}$ under varying potantials; c) transmittance versus time for switching time calculation at 630 nm (in 1 M $LiClO_4$ in PC).

Meanwhile, the PEI in PAA-PEI complexes, which is highly protonated under the film deposition conditions, introduced large amount of protons into the film. These protons increase the conductivity of the intermediate oxidized PANI,[44] thus

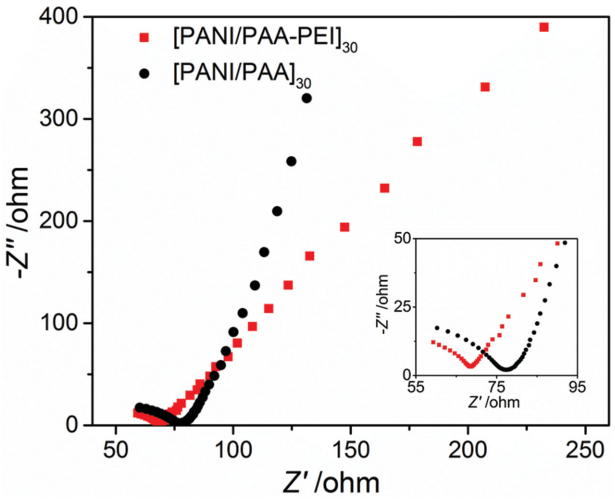

Figure 7. Nyquist plots of $[PANI/PAA\text{-}PEI]_{30}$ films and $[PANI/PAA]_{30}$ films. Insert shows the enlarged area of the high frequency region of the Nyquist plot.

also facilitates the redox reaction. EIS measurements were conducted in a frequency range of 0.1 Hz to 1 MHz. The Nyquist plots of both $[PANI/PAA]_{30}$ and $[PANI/PAA\text{-}PEI]_{30}$ films are shown in **Figure 7**. The high-frequency semicircle corresponds to the charge-transfer impedance on the electrode/electrolyte surface. The inclined line in low frequency is related to the ion diffusion process. The smaller semicircle of $[PANI/PAA\text{-}PEI]_{30}$ indicates a lower charge- transfer resistance, and a more gradual slope signifies a faster ion-diffusion process.[35] Coloration efficiency (CE) is defined by:

$$CE(\lambda) = \frac{\Delta OD}{Q}$$
$$\Delta OD(\lambda) = \log \frac{T_b}{T_c} \quad (2)$$

where Q refers to the charge inserted into the film per unit area within the coloration time, and λ is the wavelength. It represents the change in optical density (OD) per unit of charge inserted in or extracted from the film. The extracted coloration efficiency is 24.8 $cm^2\ C^{-1}$ for $[PANI/PAA\text{-}PEI]_{30}$ and 12.9 $cm^2\ C^{-1}$ for $[PANI/PAA]_{30}$ at 630 nm. A higher value of CE indicates that the $[PANI/PAA\text{-}PEI]_{30}$ film provides larger optical modulation with a smaller intercalation charge density than $[PANI/PAA]_{30}$.

3. Conclusion

In summary, stable polyelectrolyte complexes PAA-PEI were obtained and $[PANI/PAA\text{-}PEI]_n$ films were successfully fabricated via LbL assembly. The large dimensions and charge accumulation of the polyelectrolyte complex lead to a rapidly growing film with porous structure. The fast growth of the $[PANI/PAA\text{-}PEI]_n$ film enables large amount of active materials to be deposited on the substrates in a short time. Furthermore, the porous structure provides large active surface area for electrochemical reaction, shortening the ion diffusion pathway.[42]

The existence of PEI carries substantial protons under the deposition condition, contributes to the smaller charge transfer resistence and faster ion diffusion in the polyelectrolyte complexes films, thereby promotes the electrochemical reaction. Compared to $[PANI/PAA]_n$ films, $[PANI/PAA\text{-}PEI]_n$ films exhibit enhanced optical modulation and improved kinetics. It is the first time that polyelectrolyte complexes are introduced into LbL films for electrochromic studies, demonstrating that it is a facile method to use polyelectrolyte complexes as building blocks to fabricate fast growing LbL films with porous structures and enhanced electrochromism. Considering the diverse candidates for polyelectrolyte complexes, we believe that by carefully designing the composition and deposition conditions, it is promising to incorporate polyelectrolyte complexes for rapid fabrication of LbL films for various applications with controlled structures.

4. Experimental Section

Materials: Linear poly(ethylenimine) (LPEI, Mw = 25 000) was purchased from Polysciences. Poly (acrylic acid) (partially salted, Mw = 5000, 50 wt% in solution), poly(sodium-4-styrenesulfonate) (PSS, Mw ca. 70 000), polyaniline (PANI, emeraldine base, Mw ca. 5000), lithium perchlorate (≥95%), propylene carbonate (PC, anhydrous, 99.7%) and N,N-Dimethylformamide (DMF) were purchased from Sigma-Aldrich. All the chemicals were used as received. Milli-Q 18 MΩ water was used for all experiments. PH of polyelectrolyte solutions was adjusted using dilute hydrochloric acid and sodium hydroxide solutions.

Preparation of Dipping Solutions: PANI solution was made following the literature.[17,29] In short, PANI powder (100 mg) was dissolved into DMF (10 mL) and then was put in ultrasonic bath for 2 h. The solution was then stirred overnight and was filtered with 0.22 μm filter to remove big particles. After filtration, the solution was added dropwise into DI water (pH = 2.85) under vigorous stirring. The final concentration was 0.5 mg mL^{-1}. PAA-PEI complexes solution was made by slowly adding PEI solution (4 mL, 1 mg mL^{-1}, pH = 7.45) into PAA solution (30 mL, 2.3 mg mL^{-1} pH = 3.85) under stirring, which resulted in a final ratio of PAA: PEI equals to 14.7. The solution was stirred for 30 mins to obtain a stable complexes suspension. Filtration with 1 μm filter was applied before using of those complexes solutions to remove big particles if necessary. After filtration, all the complex suspensions were able to stay stable during the whole dipping process of film fabrication.

LbL Assembly of Multilayer Films: Quartz slides were treated in piranha solution (1:3 mixture of 30% H_2O_2 and 98% H_2SO_4), heating at 80 °C for 20 min. (Caution: Piranha solution reacts violently with organic material and should be handled carefully.) Indium tin oxides (ITO) coated glass slides (15 Ω sq^{-1}) were cleaned by 15 min intervals of sonication in acetone, methanol and Milli-Q water. Before assembly, ITO-glass substrates were treated by oxygen plasma for 2 min in order to get a negatively charged hydrophilic surface. To fabricate the PANI/polyelectrolyte complexes multilayer films, the freshly cleaned substrates were first immersed into PANI solution (pH = 2.85) for 10 min, followed by rinsing in pH -adjusted DI water bath (pH = 2.85). Then the substrates were immersed into polyelectrolyte complexes aqueous solution (pH = 3.85) for 5 min and rinsed in pH-adjusted DI water (pH = 3.85), resulting in a bilayer film. The procedure was repeated to *n* times to fabricate an *n* double-layer film. After assembly, the films were air-dried and then heated in the oven at 60 °C for 30 min. There was no drying step before the end of film fabrication.

Characterization: Particle size and ζ potential of the polyelectrolyte complexes were measured on a Malvin Zetasizer Nano Series 90 at room temperature. The morphology and the thickness of multilayer films were characterized and determined by field-emission scanning electron microscopy (SEM, JEOL 7600 F). Surface profiler was also used to measure the thickness of the multilayer films. The sample roughness was measured using Atomic Force Microscope (AFM) with a DI 3100 (Veeco, Digital Instruments). Ultraviolet-Visible (UV–Vis) spectra were recorded on a UV–Vis spectrophotometer (Shimadzu UV3600). The in situ spectro-electrochemical properties of individual films were carried out in a quartz cell at room temperature in the UV–Vis spectrophotometer, and the voltage supply was from Solartron 1470E. Cyclic voltammograms (CV) were performed on an electrochemical analyzer (Autolab Potentiostat, PGSTAT302N). The three-electrode cell consisted of Ag/AgCl as the reference electrode, Pt as the counter electrode and the as-synthesized LbL film on ITO-glass as the working electrode. The electrolyte used was 1 M $LiClO_4$ in PC. The electrochemical impedance spectrum (EIS) tests were conducted in the frequency range of 1 MHz to 0.1 Hz with the signal amplitude of 10 mV under open circuit voltage using Solartron 1470E.

Supporting Information

Supporting Information is available from the Wiley Online Library or from the author.

Acknowledgements

This work is conducted by NTU-HUJ-BGU Nanomaterials for Energy and Water Management Programme under the Campus for Research Excellence and Technological Enterprise (CREATE), which is supported by the National Research Foundation, Prime Minister's Office, Singapore. M. Cui acknowledges the Ph.D scholarship provided by Nanyang Technological University. The work is also supported by the A*Star – MND Green Building joint grant 1321760013.

Received: June 25, 2014
Revised: September 28, 2014
Published online: December 1, 2014

[1] a) J. Tarver, J. E. Yoo, Y. L. Loo, *Chem. Mater.* **2010**, *22*, 2333; b) C. Y. Yan, W. B. Kang, J. X. Wang, M. Q. Cui, X. Wang, C. Y. Foo, K. J. Chee, P. S. Lee, *ACS Nano* **2014**, *8*, 316.

[2] W. Kang, C. Yan, X. Wang, C. Y. Foo, A. W. Ming Tan, K. J. Zhi Chee, P. S. Lee, *J. Mater. Chem. C* **2014**, *2*, 4727.

[3] a) A. A. Argun, P. H. Aubert, B. C. Thompson, I. Schwendeman, C. L. Gaupp, J. Hwang, N. J. Pinto, D. B. Tanner, A. G. MacDiarmid, Reynolds Jr., *Chem. Mater.* **2004**, *16*, 4401; b) A. A. Argun, P. H. Aubert, B. C. Thompson, I. Schwendeman, C. L. Gaupp, J. Hwang, N. J. Pinto, D. B. Tanner, A. G. MacDiarmid, J. R. Reynolds, *Chem. Mater.* **2004**, *16*, 4401; c) G. E. Gunbas, A. Durmus, L. Toppare, *Adv. Mater.* **2008**, *20*, 691; d) A. Cihaner, F. Algi, *Adv. Funct. Mater.* **2008**, *18*, 3583; e) H. G. Wei, X. R. Yan, S. J. Wu, Z. P. Luo, S. Y. Wei, Z. H. Guo, *J. Phys. Chem. C* **2012**, *116*, 25052.

[4] a) A. Watanabe, K. Mori, Y. Iwasaki, Y. Nakamura, S. Niizuma, *Macromolecules* **1987**, *20*, 1793; b) H. G. Wei, X. R. Yan, Y. F. Li, S. J. Wu, A. Wang, S. Y. Wei, Z. H. Guo, *J. Phys. Chem. C* **2012**, *116*, 4500; c) H. G. Wei, J. H. Zhu, S. J. Wu, S. Y. Wei, Z. H. Guo, *Polymer* **2013**, *54*, 1820.

[5] K. S. Lee, G. B. Blanchet, F. Gao, Y. L. Loo, *Appl. Phys. Lett.* **2005**, *86*, 3.

[6] a) H. L. Hu, L. Hechavarria, J. Campos, *Solid State Ionics* **2003**, *161*, 165; b) M. Watanabe, M. Rikukawa, K. Sanui, N. Ogata, H. Kato, T. Kobayashi, Z. Ohtaki, *Macromolecules* **1984**, *17*, 2902.

[7] Y. Xiang, S. F. Lu, S. P. Jiang, *Chem. Soc. Rev.* **2012**, *41*, 7291.

[8] a) C. A. Nguyen, A. A. Argun, P. T. Hammond, X. H. Lu, P. S. Lee, *Chem. Mater.* **2011**, *23*, 2142; b) Z. H. Lu, M. D. Prouty, Z. H. Guo, V. O. Golub, C. Kumar, Y. M. Lvov, *Langmuir* **2005**, *21*, 2042.

[9] G. Decher, J. D. Hong, *Makromol. Chem.-Macromol. Symp.* **1991**, *46*, 321.
[10] D. Laurent, J. B. Schlenoff, *Langmuir* **1997**, *13*, 1552.
[11] D. DeLongchamp, P. T. Hammond, *Adv. Mater.* **2001**, *13*, 1455.
[12] E. Detsri, S. T. Dubas, *J. Appl. Polym. Sci.* **2013**, *128*, 558.
[13] Y. H. Chen, J. Y. Wu, Y. C. Chung, *Biosens. Bioelectron.* **2006**, *22*, 489.
[14] Z. C. Hu, J. J. Xu, Y. Tian, R. Peng, Y. Z. Xian, Q. Ran, L. T. Jin, *Electrochim. Acta* **2009**, *54*, 4056.
[15] F. Huguenin, M. Ferreira, V. Zucolotto, F. C. Nart, R. M. Torresi, O. N. Oliveira, *Chem. Mater.* **2004**, *16*, 2293.
[16] D. M. DeLongchamp, P. T. Hammond, *Chem. Mater.* **2004**, *16*, 4799.
[17] A. K. Sarker, J. D. Hong, *Langmuir* **2012**, *28*, 12637.
[18] P. T. Jia, A. A. Argun, J. W. Xu, S. X. Xiong, J. Ma, P. T. Hammond, X. H. Lu, *Chem. Mater.* **2010**, *22*, 6085.
[19] a) P. A. Chiarelli, M. S. Johal, J. L. Casson, J. B. Roberts, J. M. Robinson, H. L. Wang, *Adv. Mater.* **2001**, *13*, 1167; b) E. Kharlampieva, V. Kozlovskaya, J. Chan, J. F. Ankner, V. V. Tsukruk, *Langmuir* **2009**, *25*, 14017; c) J. Cho, K. Char, J. D. Hong, K. B. Lee, *Adv. Mater.* **2001**, *13*, 1076; d) M. Lefort, G. Popa, E. Seyrek, R. Szamocki, O. Felix, J. Hemmerle, L. Vidal, J. C. Voegel, F. Boulmedais, G. Decher, P. Schaaf, *Angew. Chem. Int. Ed.* **2010**, *49*, 10110; e) K. C. Krogman, N. S. Zacharia, S. Schroeder, P. T. Hammond, *Langmuir* **2007**, *23*, 3137; f) J. W. Jeon, J. O'Neal, L. Shao, J. Lilukenhaus, *Appl. Mater. Interfaces* **2013**, *5*, 10127.
[20] J. Seo, J. L. Lutkenhaus, J. Kim, P. T. Hammond, K. Char, *Langmuir* **2008**, *24*, 7995.
[21] a) D. L. Elbert, C. B. Herbert, J. A. Hubbell, *Langmuir* **1999**, *15*, 5355; b) P. Podsiadlo, M. Michel, J. Lee, E. Verploegen, N. W. S. Kam, V. Ball, J. Lee, Y. Qi, A. J. Hart, P. T. Hammond, N. A. Kotov, *Nano Lett.* **2008**, *8*, 1762.
[22] C. Picart, P. Lavalle, P. Hubert, F. J. G. Cuisinier, G. Decher, P. Schaaf, J. C. Voegel, *Langmuir* **2001**, *17*, 7414.
[23] C. Porcel, P. Lavalle, G. Decher, B. Senger, J. C. Voegel, P. Schaaf, *Langmuir* **2007**, *23*, 1898.
[24] Y. Li, X. Wang, J. Q. Sun, *Chem. Soc. Rev.* **2012**, *41*, 5998.
[25] a) H. M. Buchhammer, M. Mende, M. Oelmann, *Colloid Surf. A-Physicochem. Eng. Asp.* **2003**, *218*, 151; b) M. Muller, B. Kessler, S. Richter, *Langmuir* **2005**, *21*, 7044.
[26] X. K. Liu, B. Y. Dai, L. Zhou, J. Q. Sun, *J. Mater. Chem.* **2009**, *19*, 497.
[27] L. Zhang, J. Q. Sun, *Chem. Commun.* **2009**, 3901.
[28] S. Shariki, S. Y. Liew, W. Thielemans, D. A. Walsh, C. Y. Cummings, L. Rassaei, M. J. Wasbrough, K. J. Edler, M. J. Bonne, F. Marken, *J. Solid State Electrochem.* **2011**, *15*, 2675.
[29] X. Wang, K. Z. Gao, Z. Q. Shao, X. Q. Peng, X. Wu, F. J. Wang, *J. Power Sources* **2014**, *249*, 148.
[30] a) L. Zhang, M. A. Zheng, X. K. Liu, J. Q. Sun, *Langmuir* **2011**, *27*, 1346; b) S. M. Ma, X. C. Qi, Y. G. Cao, S. G. Yang, J. Xu, *Polymer* **2013**, *54*, 5382.
[31] N. Xu, X. D. Shen, S. Cui, X. B. Yi, *High Perform. Polym.* **2011**, *23*, 489.
[32] a) P. M. McManus, S. C. Yang, R. J. Cushman, *J. Chem. Soc.-Chem. Commun.* **1985**, 1556; b) J. Stejskal, P. Kratochvil, N. Radhakrishnan, *Synth. Met.* **1993**, *61*, 225.
[33] a) P. J. Yoo, K. T. Nam, J. F. Qi, S. K. Lee, J. Park, A. M. Belcher, P. T. Hammond, *Nat. Mater.* **2006**, *5*, 234; b) P. Lavalle, C. Gergely, F. J. G. Cuisinier, G. Decher, P. Schaaf, J. C. Voegel, C. Picart, *Macromolecules* **2002**, *35*, 4458.
[34] A. G. Macdiarmid, L. S. Yang, W. S. Huang, B. D. Humphrey, *Synth. Met.* **1987**, *18*, 393.
[35] G. F. Cai, J. P. Tu, D. Zhou, J. H. Zhang, Q. Q. Xiong, X. Y. Zhao, X. L. Wang, C. D. Guts, *J. Phys. Chem. C* **2013**, *117*, 15967.
[36] W. L. Liu, J. P. Tu, Y. Q. Qiao, J. P. Zhou, S. J. Shi, X. L. Wang, C. D. Gu, *J. Power Sources* **2011**, *196*, 7728.
[37] H. Y. Zhang, X. J. Yan, Y. W. Wang, Y. H. Deng, X. G. Wang, *Polymer* **2008**, *49*, 5504.
[38] S. I. Cho, W. J. Kwon, S. J. Choi, P. Kim, S. A. Park, J. Kim, S. J. Son, R. Xiao, S. H. Kim, S. B. Lee, *Adv. Mater.* **2005**, *17*, 171.
[39] X. H. Xia, J. P. Tu, J. Zhang, X. L. Wang, W. K. Zhang, H. Huang, *Nanotechnology* **2008**, *19*, 7.
[40] M. K. Ram, E. Maccioni, C. Nicolini, *Thin Solid Films* **1997**, *303*, 27.
[41] D. T. Ge, L. L. Yang, Z. Q. Tong, Y. B. Ding, W. H. Xin, J. P. Zhao, Y. Li, *Electrochim. Acta* **2013**, *104*, 191.
[42] a) S. Bhandari, M. Deepa, A. K. Srivastava, A. G. Joshi, R. Kant, *J. Phys. Chem. B* **2009**, *113*, 9416; b) J. Vaillant, M. Lira-Cantu, K. Cuentas-Gallegos, N. Casan-Pastor, P. Gomez-Romero, *Prog. Solid State Chem.* **2006**, *34*, 147.
[43] a) E. T. Kang, K. G. Neoh, K. L. Tan, *Prog. Polym. Sci.* **1998**, *23*, 277; b) W. S. Huang, B. D. Humphrey, A. G. Macdiarmid, *J. Chem. Soc. Faraday Trans. I* **1986**, *82*, 2385.
[44] a) X. H. Xia, J. P. Tu, Y. J. Mai, R. Chen, X. L. Wang, C. D. Gu, X. B. Zhao, *Chem. Eur. J.* **2011**, *17*, 10898; b) R. D. Armstrong, H. Wang, *Electrochim. Acta* **1991**, *36*, 759.